

TeV SUSY dark matter confronted with the current direct and indirect detection data

Murat Abdughani^{1,2}, Jie Ren^{1,2}, Jun Zhao^{1,2,3},

¹ *CAS Key Laboratory of Theoretical Physics, Institute of Theoretical Physics, Chinese Academy of Sciences, Beijing 100190, China*

² *School of Physical Sciences, University of Chinese Academy of Sciences, Beijing 100049, China*

³ *Institute of Theoretical Physics, College of Applied Science, Beijing University of Technology, Beijing 100124, China*

Abstract

In the minimal supersymmetric standard model (MSSM) the lightest superparticle (LSP) can be a TeV neutralino (mainly dominated by higgsino or wino) which serves as a dark matter candidate with correct thermal relic density. In this work we confront the 1-2 TeV neutralino dark matter with the latest direct and indirect detections from PandaX and AMS-02/DAMPE. Considering various scenarios with decoupled sfermions, with A -mediated annihilation, with squark or stop coannihilation, we find that the parameter space is stringently constrained by the direct detection limits. In the allowed parameter space, the TeV neutralino dark matter annihilation contribution to the anti-proton flux is found to agree with the AMS-02 data while its contribution to electron/positron flux is too small to cause any visible excess. The current survived parameter space can be mostly covered by the future direct detection experiment LZ7.2T.

I. INTRODUCTION

Identifying the nature of the cosmic dark matter is a primary topic in today's particle physics and cosmology. In the popular minimal supersymmetric standard model (MSSM), the lightest neutralino is a natural candidate for the cosmic cold dark matter. In general, a neutralino dark matter with a mass around 100 GeV (a typical WIMP) can be effectively explored at direct detection experiments and the LHC. However, a neutralino dark matter above TeV scale or below GeV scale is hard to detect at the LHC. On the other hand, the current direct detections [1] have relatively low sensitivities to such a super-heavy or ultra-light neutralino dark matter and hence the limits on their interactions with the nucleon are rather weak. For the TeV scale dark matter, another motivation comes from the recent DAMPE observation [2] of a plausible electron/positron excess at TeV energy which may indicate a heavy dark matter at TeV scale. Theoretically, in the MSSM an ultra-light GeV scale neutralino dark matter can only be achieved in some unnatural limits (say the alignment limit without decoupling [3, 4]), but a TeV scale neutralino dark matter can be naturally obtained with correct thermal relic density. So a TeV scale neutralino dark matter is an interesting scenario to study.

Such a TeV neutralino dark matter has been discussed in the literature [5–16]. In this work we intend to give a more complete study by considering various scenarios with decoupled sfermions, with A -mediated annihilation, with squark or stop coannihilation. Under the requirement of giving correct thermal relic density, we will show its components. Then we will demonstrate the constraints of the latest direct detections on its parameter space. In the allowed parameter space we will show the contributions of its annihilation to the anti-proton and electron/positron cosmic-ray fluxes, which will be compared with the AMS-02 and DAMPE data.

The structure of this paper is organized as follows. In Section II we show the scenarios and the components of the TeV neutralino dark matter under the requirement of giving correct thermal relic density. In Section III we confront the TeV neutralino dark matter in various scenarios with the latest direct detection limits from PandaX and indirect constraints from the anti-proton and electron/positron cosmic-ray fluxes from AMS-02 and DAMPE data. Finally, we draw our conclusions in Section IV.

II. TEV NEUTRALINO DARK MATTER WITH CORRECT RELIC DENSITY

In the MSSM the two neutral higgsinos (\tilde{H}_u^0 and \tilde{H}_d^0) and the two neutral gauginos (\tilde{B} and \tilde{W}^0) are mixed to form four mass eigenstates called neutralinos. In the gauge-eigenstate basis ($\tilde{B}, \tilde{W}^0, \tilde{H}_d, \tilde{H}_u$), the neutralinos are defined as $\tilde{\chi}_i^0 = Z_N^{ij}(\tilde{B}, \tilde{W}^0, \tilde{H}_d, \tilde{H}_u)$ while the charginos are defined as $\tilde{\chi}_i^\pm = Z_\pm^{ij}(\tilde{W}^\pm, \tilde{H}^\pm)$, where $\tilde{B}, \tilde{W}, \tilde{H}_d, \tilde{H}_u$ are respectively the bino, wino, and higgsino fields, and Z_N^{ij} and Z_\pm^{ij} are neutralino and chargino mixing matrices.

In our analysis we take the bino mass M_1 , wino mass M_2 , and higgsino mass μ in the range of 1-7 TeV when we scan over the parameter space. We require the neutralino dark matter (the lightest neutralino) in the range of 1-2 TeV. In our scan we use MicrOEMGAs [17] to calculate the thermal relic density $\Omega_{\tilde{\chi}} h^2$ and the cross sections and require the neutralino dark matter to provide the relic density in the 2σ range of the measured value [18]. We fix $\tan\beta = 30$ and trilinear terms $A_i = 0$. We consider the following scenarios:

- (i) **Decoupled Case:** Motivated from the split supersymmetry [19], in this case we set sfermion mass parameters and the CP-odd Higgs mass as heavy as 10 TeV to decouple them from gauginos. In this case the main processes which affect the dark matter relic density and annihilation cross section involve the interactions between neutralinos, charginos and the W/Z or Higgs boson. The interactions of gauge boson with neutralino and chargino are given by (we used the conventions in [20] for particles, couplings, and their diagonalization matrices)

$$\begin{aligned}
& \frac{e}{s_W} \bar{\chi}_j \gamma^\mu \left[(Z_N^{2i} Z_+^{1j*} - \frac{1}{\sqrt{2}} Z_N^{4i} Z_+^{2j*}) P_L + (Z_N^{2i*} Z_-^{1j} + \frac{1}{\sqrt{2}} Z_N^{3i*} Z_-^{2j}) P_R \right] \chi_i^0 W_\mu^+ \\
& - \frac{e}{2s_W c_W} \bar{\chi}_i \gamma^\mu (Z_+^{1i*} Z_+^{1j} P_L + Z_-^{1i} Z_-^{1j*} P_R + (c_W^2 - s_W^2) \delta^{ij}) \chi_j Z_\mu \\
& + \frac{e}{4s_W c_W} \bar{\chi}_i^0 \gamma^\mu ((Z_N^{4i*} Z_N^{4j} - Z_N^{3i*} Z_N^{3j}) P_L - (Z_N^{4i} Z_N^{4j*} - Z_N^{3i} Z_N^{3j*}) P_R) \chi_j^0 Z_\mu
\end{aligned} \tag{1}$$

The interactions of Higgs boson with neutralino and chargino are given by

$$\begin{aligned}
& \frac{e}{2s_W c_W} \bar{\chi}_i^0 [(Z_R^{1k} Z_N^{3j} - Z_R^{2k} Z_N^{4j})(Z_N^{1i} s_W - Z_N^{2i} c_W) P_L \\
& + (Z_R^{1k} Z_N^{3i*} - Z_R^{2k} Z_N^{4i*})(Z_N^{1j*} s_W - Z_N^{2j*} c_W) P_R] \chi_j^0 H_k^0 \\
& - \frac{e}{\sqrt{2}s_W} \bar{\chi}_i [(Z_R^{1k} Z_-^{2i} Z_+^{1j} + Z_R^{2k} Z_-^{1i} Z_+^{2j}) P_L \\
& + (Z_R^{1k} Z_-^{2j*} Z_+^{1i*} + Z_R^{2k} Z_-^{1j*} Z_+^{2i*}) P_R] \chi_j H_k^0
\end{aligned} \tag{2}$$

We know from the above equations that the pure bino does not interact with gauge boson or Higgs boson. So the bino LSP annihilation can only proceed through coannihilation or mixing with higgsino or wino. Thus the bino dark matter annihilation cross section is smaller than higgsino and wino dark matter.

- (ii) **A-mediated Case:** In this case the LSP dark matter annihilates through the s -channel resonance of the CP-odd Higgs boson A , usually called "A-funnel" [21]. Here we decouple all sfermions (fix them to 10 TeV) and consider the resonance of A which enhances the annihilation of dark matter. The relevant interactions for the A -funnel annihilation processes are given by

$$\begin{aligned}
& \frac{ie}{\sqrt{2}s_W} \bar{\chi}_i \left[(Z_H^{1k} Z_-^{2i} Z_+^{1j} + Z_H^{2k} Z_-^{1i} Z_+^{2j}) P_L - (Z_H^{1k} Z_-^{2j^*} Z_+^{1i^*} + Z_H^{2k} Z_-^{1j^*} Z_+^{2i^*}) P_R \right] \chi_j A_k^0 \\
& - \frac{ie}{2s_W c_W} \bar{\chi}_i^0 \left[(Z_H^{1k} Z_N^{3j} - Z_H^{2k} Z_N^{4j}) (Z_N^{1i} s_W - Z_N^{2i} c_W) P_L \right. \\
& \left. - (Z_H^{1k} Z_N^{3i^*} - Z_H^{2k} Z_N^{4i^*}) (Z_N^{1j^*} s_W - Z_N^{2j^*} c_W) P_R \right] \chi_j^0 A_k^0
\end{aligned} \tag{3}$$

- (iii) **Coannihilation Cases:** When a squark or stop has a mass approaching the LSP, it coannihilates with the LSP and helps to achieve the correct relic density. In both cases (squark coannihilation and stop coannihilation) we fix A mass at 10 TeV. For squark (stop) coannihilation, the squark (stop) mass is required to within 120% of the LSP mass. The relevant interactions for squark coannihilation are given by

$$\begin{aligned}
& U_i^- \bar{\chi}_1^0 \left[\left(\frac{-e}{\sqrt{2}s_W c_W} Z_U^{Ii^*} \left(\frac{1}{3} Z_N^{11} s_W + Z_N^{21} c_W \right) - Y_u^I Z_U^{(I+3)1^*} Z_N^{41} \right) P_L \right. \\
& \left. + \left(\frac{2e\sqrt{2}}{3c_W} Z_U^{(I+3)i^*} Z_N^{11^*} - Y_u^I Z_U^{Ii^*} Z_N^{41^*} \right) P_R \right] u^I + \text{H.c.} \\
& + D_i^+ \bar{\chi}_1^0 \left[\left(\frac{-e}{\sqrt{2}s_W c_W} Z_D^{Ii} \left(\frac{1}{3} Z_N^{11} s_W - Z_N^{21} c_W \right) + Y_d^I Z_D^{(I+3)i} Z_N^{31} \right) P_L \right. \\
& \left. + \left(\frac{-e\sqrt{2}}{3c_W} Z_D^{(I+3)i} Z_N^{11^*} + Y_d^I Z_D^{Ii} Z_N^{31^*} \right) P_R \right] d^I + \text{H.c.}
\end{aligned} \tag{4}$$

In Fig. 1 we show the components of the TeV neutralino dark matter under the requirement of correct thermal relic density. We see that in all four cases the TeV neutralino dark matter is dominated by higgsino or wino in order to satisfy the relic density. Actually, a pure higgsino (wino) dark matter around 1.1 (2.1) TeV has been found to give the required

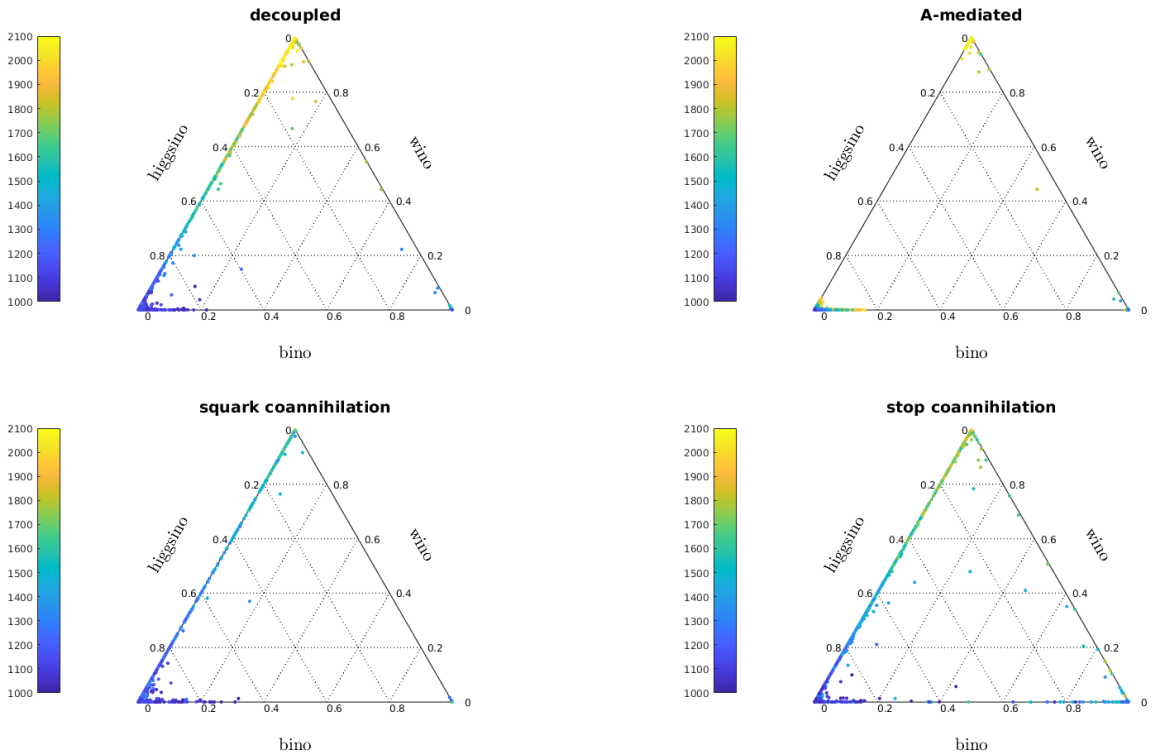


FIG. 1. Scatter plots of the TeV neutralino dark matter showing the components under the requirement of thermal relic density. The colors denote the dark matter mass from 1 TeV to 2.1 TeV.

thermal relic density in the literature [8, 22, 23]. The number of bino-like samples is quite small in the decoupled scenario, but increases in the A-mediation and squark coannihilation cases, as expected.

III. CONSTRAINTS FROM DARK MATTER DETECTIONS

The on-going direct and indirect detection experiments have constrained the dark matter interactions with the standard model (SM) particles. In Fig. 2, the upper panels show the spin-independent neutralino-nucleon scattering cross sections where the current upper limits from PandaX and the future sensitivity of LZ7.2T are plotted. We see that the current PandaX data has excluded the region where higgsino and wino are mixed. The future LZ7.2T experiment can cover the whole higgsino region and a major part of the wino region.

The lower panels of Fig. 2 show the neutralino dark matter annihilation cross sections

where the upper limits from the AMS-02 anti-proton data and the Fermi-LAT γ -ray data [24] from the observation of dwarf spheroidal galaxies are plotted. We see that the upper limits from these indirect detection data are weaker than the direct detection limits (the parameter space above the AMS-02 anti-proton limits has already been excluded by the PandaX data).

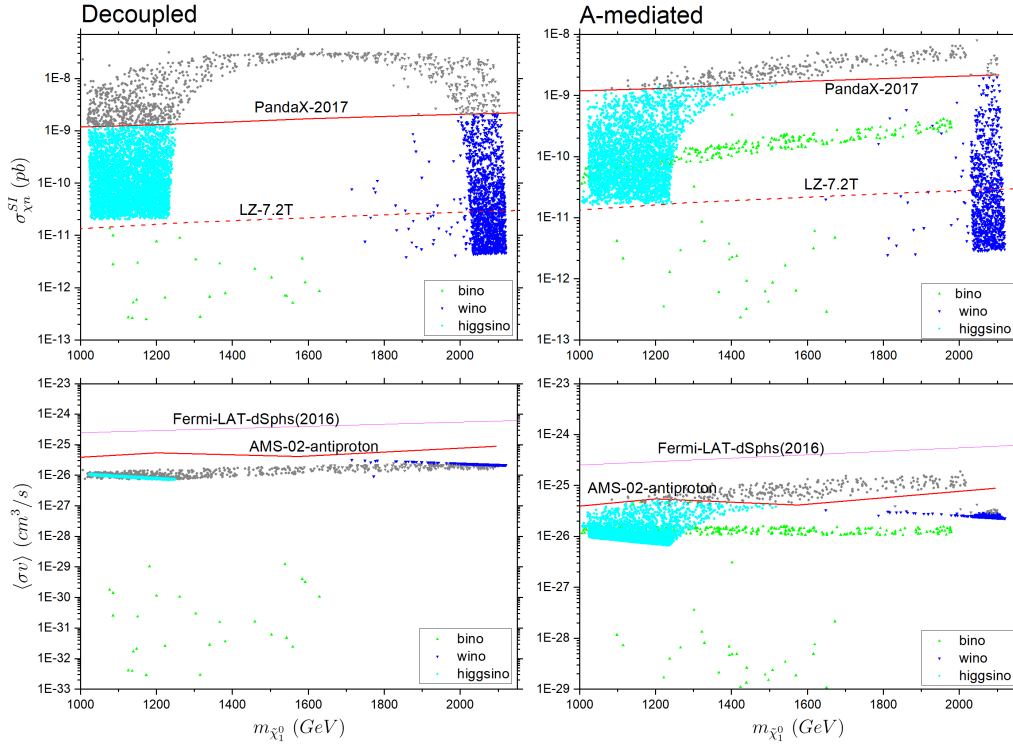


FIG. 2. Scatter plots of parameter space satisfying the relic density at 2σ level. The left panels are for the decoupled case while the right panels are for the A -mediated case. The upper parts show the spin-independent neutralino LSP-nucleon scattering cross sections where the curves are the 90% CL upper limits from PandaX (2017) [1] and the future sensitivity from LZ7.2T. The lower parts show the dark matter annihilation cross sections $\langle\sigma v\rangle$ where the curves are the 95% CL upper limits from the AMS-02 anti-proton data [25] and the Fermi-LAT γ -ray data (dwarf spheroidal galaxies) [24]. The bino, wino and higgsino samples represent bino-like, wino-like and higgsino-like LSP, respectively.

In our calculation of the electron/positron and antiproton flux from the dark matter halo, we changed the energy spectrum of dark matter source term in GALPROP [26]. This source

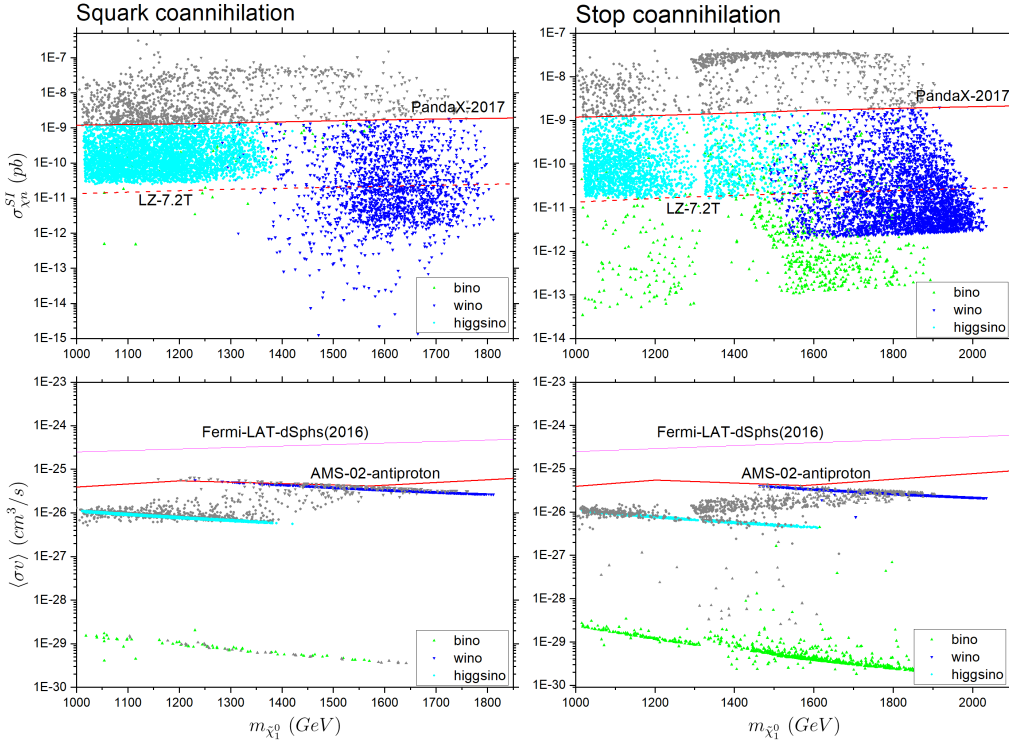


FIG. 3. Same as Fig. 2, but for squark and stop coannihilation cases.

term is

$$q_{\bar{p}, e^\pm}^{DM}(\mathbf{x}, E_{kin}) = \frac{1}{2} \left(\frac{\rho(\mathbf{x})}{m_{DM}} \right)^2 \sum_f \langle \sigma v \rangle_f \frac{dN_{\bar{p}, e^\pm}^f}{dE_{kin}} \quad (5)$$

where \bar{p}, e^\pm are antiproton and electron/positron, $\rho(\mathbf{x})$ is the dark matter density distribution, m_{DM} is the dark matter mass, $\langle \sigma v \rangle_f$ is thermally averaged cross section for dark matter annihilation into the SM final state f ($DM + DM \rightarrow f\bar{f}$), $dN_{\bar{p}, e^\pm}^f/dE_{kin}$ are the antiproton and electron/positron energy spectrum per annihilation, and the factor 1/2 is for the Majorana dark matter fermion. For $\rho(\mathbf{x})$ we use NFW dark matter density profile [27]

$$\rho_{NFW}(r) = \rho_0 \frac{r_0}{r} \left(\frac{r_0}{r_0 + r} \right)^2 \quad (6)$$

with the halo radius 20 kpc, the local dark matter density $\rho_0 = 0.43 \text{ GeV}/\text{cm}^3$ [28] at the solar position $r_0 = 8 \text{ kpc}$.

From the source term we know that m_{DM} and $\langle \sigma v \rangle_F$ are crucial for the intensity of the flux and, therefore, we here choose one benchmark point for each case. The energy spectrum $dN_{\bar{p}, e^\pm}^f/dE_{kin}$ data from [29] are used with the interpolation method for the source term in

TABLE I. Four benchmark points, one point for each case (decoupled case, A -mediated case, squark and stop coannihilation cases) with largest $\langle\sigma v\rangle$.

m_{DM}	$\langle\sigma v\rangle$	Final states ($f\bar{f}$)					DM components			
		W^+W^-	Z^+Z^-	$\tau^+\tau^-$	$b\bar{b}$	$t\bar{t}$	Z_N^{11}	Z_N^{12}	Z_N^{13}	Z_N^{14}
1463.6	$4.61 \times 10^{\hat{(-26)}}$	0.8730	0.1260	0	0	0	0.0012	-0.9978	0.0557	-0.0361
994.30	$1.36 \times 10^{\hat{(-26)}}$	0.6570	0.2180	0	0	0.0740	0.2639	-0.3153	0.6531	-0.6359
1714.9	$3.18 \times 10^{\hat{(-26)}}$	0.9999	0	0	0	0	0.1369	-0.99	0.0312	-0.0161
1267.1	$5.01 \times 10^{\hat{(-26)}}$	0.0720	0.0530	0.1150	0.7300	0.0139	0.1619	-0.0172	0.6993	-0.6960

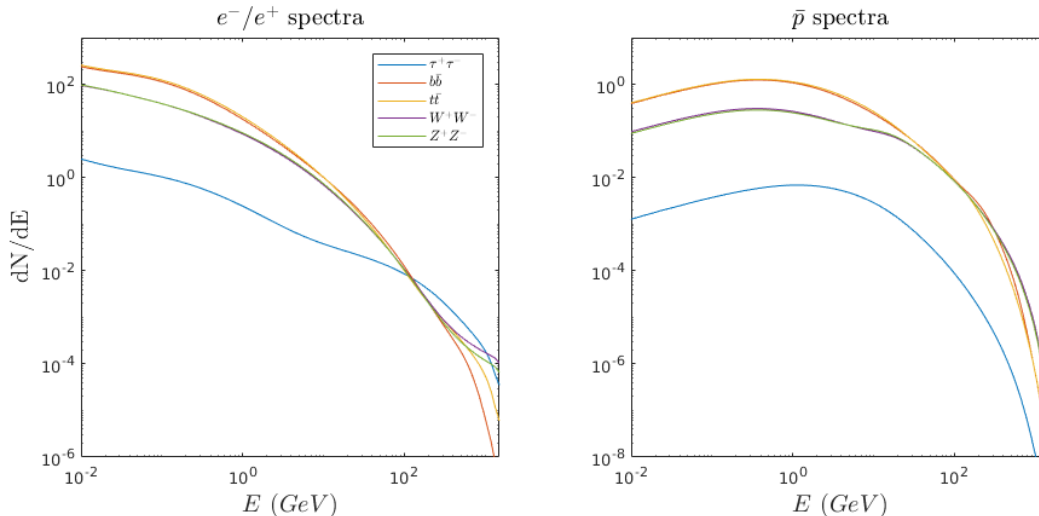


FIG. 4. The positron/electron and antiproton spectra produced by the annihilation of two dark matter particles with mass 1.5 TeV.

GALPROP. In the 1-2 TeV dark matter mass range, the spectra of e^\pm , \bar{p} are similar and thus we only show the spectra for $m_{DM} = 1.5$ TeV in Fig. 4. Also, we display in Table I four benchmark points, one point for each case with largest $\langle\sigma v\rangle$.

Fig. 5 is the antiproton and electron plus positron flux calculated by GALPROP, compared with the experimental data. Here we see that the contributions of the 1-2 TeV neutralino dark matter annihilation are too small to cause visible excess. This means that the plausible electron/positron cosmic-ray excess at TeV energy reported by DAMPE [2] is not likely from the TeV neutralino dark matter annihilation. If this excess is verified, it may point to some TeV leptophilic dark matter [34]. However, the small contribution to the

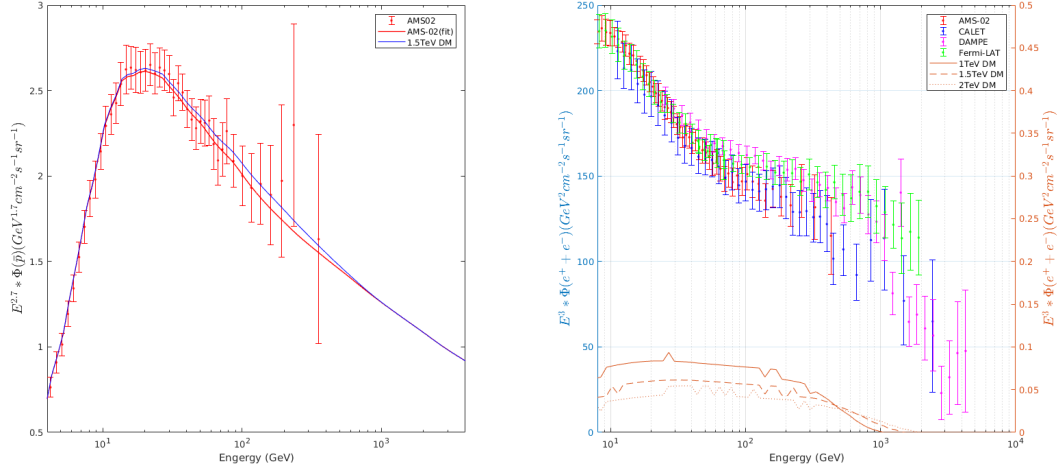


FIG. 5. The antiproton flux (left panel) and electron plus positron flux (right panel). For the antiproton flux, the AMS-02 data [30] and its fitted curve as well as the results with the 1.5 TeV neutralino dark matter annihilation contribution are shown. For the electron plus positron flux, the AMS-02 [31], the CALET [32], the DAMPE [2] and the Fermi-LAT [33] data (read the left Y-axis) as well as the 1-2 TeV neutralino dark matter annihilation contribution (read the right Y-axis) are shown. The errors of the data are 1σ statistical and systematic.

antiproton flux from the TeV neutralino dark matter annihilation is still favored because so far no excess has been observed for the antiproton flux.

In summary, the 1-2 TeV neutralino dark matter with correct thermal relic density has been stringently constrained by the direct detection data. The constraints of indirect detections from cosmic-ray flux are much weaker than direct detection limits. The survived parameter space can be mostly covered by the future direct detection experiment LZ7.2T. At the colliders, the TeV neutralino dark matter is hard to probe at the LHC [35], but can be effectively probed at a 100 TeV hadron collider. For example, for a luminosity of 3000 fb^{-1} , a 100 TeV hadron collider can give a good probe for a TeV higgsino in the decoupled case [36] and 1-3 TeV for stop coannihilation case [37].

IV. CONCLUSION

In this work we examined the thermal neutralino dark matter in a mass range of 1-2 TeV. We considered various scenarios and confronted them with the latest direct and

indirect detections from PandaX and AMS-02/DAMPE. We observed that the parameter space is stringently constrained by the direct detection limits. In the allowed parameter space, the 1-2 TeV neutralino dark matter annihilation contribution to the anti-proton flux is found to agree with the AMS-02 data while its contribution to electron/positron flux is too small to cause any visible excess. The current survived parameter space can be mostly covered by a future direct detection experiment LZ7.2T.

ACKNOWLEDGEMENT

This work was supported by the National Natural Science Foundation of China (NNSFC) under grant Nos. 11705093, 11305049, 11675242 and 11375001, by Peng-Huan-Wu Theoretical Physics Innovation Center (11747601), by the CAS Center for Excellence in Particle Physics (CCEPP), by the CAS Key Research Program of Frontier Sciences and by a Key R&D Program of Ministry of Science and Technology of China under number 2017YFA0402200-04.

-
- [1] X. Cui *et al.* (PandaX-II), *Phys. Rev. Lett.* **119**, 181302 (2017), [arXiv:1708.06917 \[astro-ph.CO\]](#).
 - [2] G. Ambrosi *et al.* (DAMPE), *Nature* **552**, 63 (2017), [arXiv:1711.10981 \[astro-ph.HE\]](#).
 - [3] G. H. Duan, W. Wang, L. Wu, J. M. Yang, and J. Zhao, *Phys. Lett.* **B778**, 296 (2018), [arXiv:1711.03893 \[hep-ph\]](#).
 - [4] J. Ren, L. Wu, J. M. Yang, and J. Zhao, (2017), [arXiv:1708.06615 \[hep-ph\]](#).
 - [5] M. Beneke, A. Bharucha, F. Dighera, C. Hellmann, A. Hryczuk, S. Recksiegel, and P. Ruiz-Femenia, *JHEP* **03**, 119 (2016), [arXiv:1601.04718 \[hep-ph\]](#).
 - [6] M. Beneke, A. Bharucha, A. Hryczuk, S. Recksiegel, and P. Ruiz-Femenia, *JHEP* **01**, 002 (2017), [arXiv:1611.00804 \[hep-ph\]](#).
 - [7] M. Abdughani, L. Wu, and J. M. Yang, *Eur. Phys. J.* **C78**, 4 (2018), [arXiv:1705.09164 \[hep-ph\]](#).
 - [8] J. Bramante, N. Desai, P. Fox, A. Martin, B. Ostdiek, and T. Plehn, *Phys. Rev.* **D93**, 063525 (2016), [arXiv:1510.03460 \[hep-ph\]](#).

- [9] G. H. Duan, K.-I. Hikasa, J. Ren, L. Wu, and J. M. Yang, (2018), [arXiv:1804.05238 \[hep-ph\]](#).
- [10] C. Han, J. Ren, L. Wu, J. M. Yang, and M. Zhang, *Eur. Phys. J.* **C77**, 93 (2017), [arXiv:1609.02361 \[hep-ph\]](#).
- [11] A. Kobakhidze, M. Talia, and L. Wu, *Phys. Rev.* **D95**, 055023 (2017), [arXiv:1608.03641 \[hep-ph\]](#).
- [12] N. Liu and L. Wu, *Eur. Phys. J.* **C77**, 868 (2017), [arXiv:1705.02534 \[hep-ph\]](#).
- [13] C. Han, K.-i. Hikasa, L. Wu, J. M. Yang, and Y. Zhang, *Phys. Lett.* **B769**, 470 (2017), [arXiv:1612.02296 \[hep-ph\]](#).
- [14] G. Grilli di Cortona, *JHEP* **05**, 035 (2015), [arXiv:1412.5952 \[hep-ph\]](#).
- [15] K. Kowalska and E. M. Sessolo (2018) [arXiv:1802.04097 \[hep-ph\]](#).
- [16] A. Mitridate, M. Redi, J. Smirnov, and A. Strumia, *JCAP* **1705**, 006 (2017), [arXiv:1702.01141 \[hep-ph\]](#).
- [17] G. Belanger, F. Boudjema, A. Pukhov, and A. Semenov, *Comput. Phys. Commun.* **185**, 960 (2014), [arXiv:1305.0237 \[hep-ph\]](#).
- [18] P. A. R. Ade *et al.* (Planck), *Astron. Astrophys.* **571**, A16 (2014), [arXiv:1303.5076 \[astro-ph.CO\]](#).
- [19] J. D. Wells, in *11th International Conference on Supersymmetry and the Unification of Fundamental Interactions (SUSY 2003) Tucson, Arizona, June 5-10, 2003* (2003) [arXiv:hep-ph/0306127 \[hep-ph\]](#).
- [20] J. Rosiek, (1995), [arXiv:hep-ph/9511250 \[hep-ph\]](#).
- [21] S. P. Martin, *Phys. Rept.* **175**, 1 (1997), [Adv. Ser. Direct. High Energy Phys.18,1(1998)], [arXiv:hep-ph/9709356 \[hep-ph\]](#).
- [22] T. Cohen, M. Lisanti, A. Pierce, and T. R. Slatyer, *JCAP* **1310**, 061 (2013), [arXiv:1307.4082 \[hep-ph\]](#).
- [23] J. Fan and M. Reece, *JHEP* **10**, 124 (2013), [arXiv:1307.4400 \[hep-ph\]](#).
- [24] A. Albert *et al.* (DES, Fermi-LAT), *Astrophys. J.* **834**, 110 (2017), [arXiv:1611.03184 \[astro-ph.HE\]](#).
- [25] A. Cuoco, J. Heisig, M. Korsmeier, and M. Krmer, (2017), [arXiv:1711.05274 \[hep-ph\]](#).
- [26] A. W. Strong, I. V. Moskalenko, and O. Reimer, *Astrophys. J.* **537**, 763 (2000), [Erratum: *Astrophys. J.*541,1109(2000)], [arXiv:astro-ph/9811296 \[astro-ph\]](#).

- [27] J. F. Navarro, C. S. Frenk, and S. D. M. White, *Astrophys. J.* **462**, 563 (1996), [arXiv:astro-ph/9508025 \[astro-ph\]](#).
- [28] P. Salucci, F. Nesti, G. Gentile, and C. F. Martins, *Astron. Astrophys.* **523**, A83 (2010), [arXiv:1003.3101 \[astro-ph.GA\]](#).
- [29] M. Cirelli, G. Corcella, A. Hektor, G. Hutsi, M. Kadastik, P. Panci, M. Raidal, F. Sala, and A. Strumia, *JCAP* **1103**, 051 (2011), [Erratum: *JCAP*1210,E01(2012)], [arXiv:1012.4515 \[hep-ph\]](#).
- [30] M. Aguilar *et al.* (AMS), *Phys. Rev. Lett.* **117**, 091103 (2016).
- [31] M. Aguilar *et al.* (AMS), *Phys. Rev. Lett.* **113**, 121102 (2014).
- [32] O. Adriani *et al.* (CALET), *Phys. Rev. Lett.* **119**, 181101 (2017), [arXiv:1712.01711 \[astro-ph.HE\]](#).
- [33] S. Abdollahi *et al.* (Fermi-LAT), *Phys. Rev.* **D95**, 082007 (2017), [arXiv:1704.07195 \[astro-ph.HE\]](#).
- [34] G. H. Duan, L. Feng, F. Wang, L. Wu, J. M. Yang, and R. Zheng, *JHEP* **02**, 107 (2018), [arXiv:1711.11012 \[hep-ph\]](#).
- [35] C. Han, A. Kobakhidze, N. Liu, A. Saavedra, L. Wu, and J. M. Yang, *JHEP* **02**, 049 (2014), [arXiv:1310.4274 \[hep-ph\]](#).
- [36] M. Low and L.-T. Wang, *JHEP* **08**, 161 (2014), [arXiv:1404.0682 \[hep-ph\]](#).
- [37] T. Cohen, R. T. D’Agnolo, M. Hance, H. K. Lou, and J. G. Wacker, *JHEP* **11**, 021 (2014), [arXiv:1406.4512 \[hep-ph\]](#).